Femtosecond laser highly-efficient plane processing based on an axicon-generated donut-shaped beam

Zhi Luo (罗 志), Cong Wang (王 聪), Xinran Dong (董欣然)*, and Ji'an Duan (段吉安)**

State Key Laboratory of High Performance and Complex Manufacturing, Central South University, Changsha 410083, China

**Corresponding author: xrdong@csu.edu.cn; **corresponding author: duanjian@csu.edu.cn*

Received September 20, 2017; accepted January 4, 2018; posted online March 2, 2018

A simple technique is proposed for highly-efficient plane processing fully based on femtosecond laser beam shaping. The laser intensity distribution is transformed from a Gaussian to a donut shape. As the donut-shaped focus seems like a flat top from the side view, a plane with a high level of flatness is obtained directly by scanning once. By applying it to polishing experiments, the surface roughness can be improved significantly. The influence of scanning speed, laser pulse energy, and scanning times on the roughness is also discussed. Moreover, the scanning width can be flexibly controlled in a wide range.

OCIS codes: 140.7090, 140.3300, 240.5450.
doi: 10.3788/COL201816.031401.

An axicon is a specialized type of lens, which has a conical surface and is defined by its apex angle. Unlike a converging lens, which is designed to focus a light source to a spot, the axicon focuses a light source to a line along the optical axis[1–3]. Also, axicons are less prone to aberrations. Moreover, the axicon-generated focal line can be approximated by a zero-order Bessel-type beam[4,5]. In doing so, a beam generated by an axicon has wide applications in the fields of imaging[6–8], optical coherence tomography[9], optical micromanipulation[10], optical tweezers[11], and especially in the field of ultrafast laser micro-/nano-fabrication, which can produce micro-holes/micro-channels with a very high aspect ratio[12,13].

In addition to the focal line, a donut focus can also be generated by using an axicon, which will be discussed in this Letter and be used for femtosecond (fs) laser highly-efficient plane processing. Traditionally, during fs laser fabrication[14–16], a lens or an objective is applied to focusing the laser into a tiny spot. Then, a three-dimensional translation stage is indispensable in the fabrication process to move samples relative to the focus to connect processed dots into a line and lines into a plane[17,18]. Therefore, it is extremely time-consuming for large-area fabrications and only suitable for the laser system with a high pulse repetition frequency (PRF) (≥100 kHz). However, if a donut focus is employed, the efficiency will be improved significantly, as a plane will directly form with just one scanning. This makes it possible for a laser system with a low PRF to fabricate a plane efficiently. For example, in the field of laser cleaning, in contrast to traditional technology, a high-speed galvanometer scanning system has to be used to create a line-focus in the lateral direction by connecting lots of processed dots[19,20]; the donut-shaped beam itself is just a line-focus from the side view. Therefore, the efficiency can be improved dramatically by using a donut focus, so it has a potential application in the field of laser cleaning. In this Letter, highly-efficient plane processing by a fs laser with a low PRF is demonstrated based on shaping a Gaussian beam into a donut shape. With the donut-shaped beam, experiments of fs laser polishing are performed. It shows that the processed surface keeps a relatively high level of flatness, and the surface roughness is improved significantly. Moreover, the influence of scanning speed, laser pulse energy, and scanning times on the surface roughness is also studied in this work.

Typically, a quasi-Bessel beam will be generated first after an axicon, as shown in Fig. 1(a), which illustrates the geometrical evolution of a Gaussian beam converted to a donut-shaped beam. From the image, it can be seen that a ring-like beam is formed after the Bessel area. The diameter of the ring is proportional to the distance from the axicon output to the imaging position, while the ring thickness maintains a constant value. To understand the highly-efficient plane processing with the proposed method, we first perform numerical simulations to compare the spatial intensity distribution between a donut-shaped beam and a cylindrical lens created transverse line-focus beam, which is selected for comparison since it can also achieve highly-efficient fabrication with one scanning. Figures 1(c) and 1(e) show the top view and side view of the spatial intensity distribution of a donut-shaped beam, respectively. It is obtained from the mathematical model[21],

$$I(r,Z) = I_0 \frac{A + (Z \times \theta) - r}{r} \left(\frac{\omega_0}{\omega_z}\right)^2 \times \exp\left\{-\frac{2[A + (Z \times \theta) - r]^2}{\omega_z^2}\right\}, \quad (1)$$

where r is the radial distance in cylindrical coordinates, Z is the distance from the end point of the Bessel area, A is the beam radius of the incident light, I_0 is the on-axis field amplitude, ω_0 is the waist radius of the input Gaussian beam, ω_z is the radius of the Gaussian beam at the

 © 2018 Chinese Optics Letters

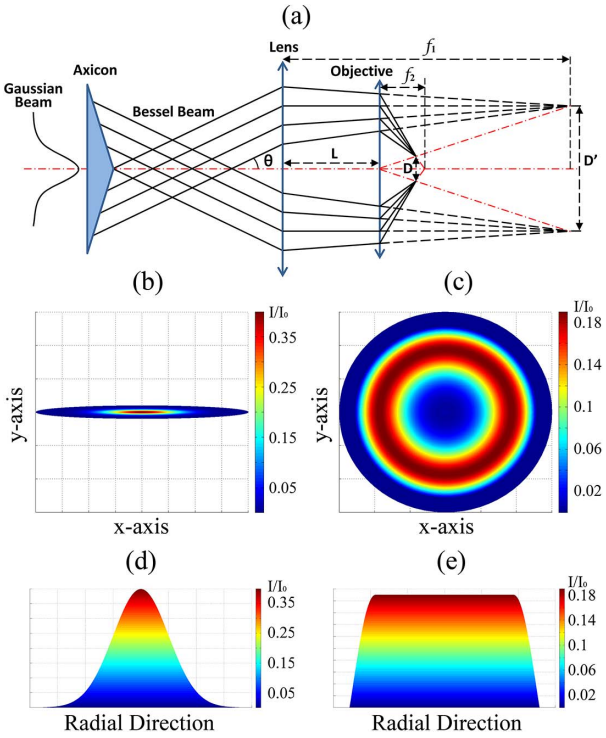

Fig. 1. (a) Geometrical evolution from a Gaussian beam to a donut-shaped beam. (b),(d) The top view and side view of a beam focused by a cylindrical lens. (c),(e) The top view and side view of a donut-shaped beam formed with an axicon.

position of z, and θ is the angle with a vector normal to the conical surface of wavefront included with the z axis.

Figures 1(b) and 1(d) show the top view and side view of the spatial intensity distribution of a beam focused by a cylindrical lens. It can be clearly seen that most of the laser energy still gathers in the central area despite a transverse line-focus formed with a cylindrical lens. However, for the donut-shaped beam shown in Fig. 1(c), the central laser intensity is evenly distributed along the ring. Moreover, as shown in Fig. 1(e), it seems like a flat-top beam from the side view. Therefore, it is a favorable choice for plane processing. Below, we will perform experiments to compare machined results by the donut-shaped beam and the cylindrical lens focused beam.

For the setup used in this work, the laser source is a Ti: sapphire amplified fs laser system. The output beam has a pulse duration of 120 fs, a wavelength of 800 nm, a pulse repetition rate of 1 kHz, and a horizontal polarization, and the original beam has a fundamental transverse Gaussian mode (TEM_{00}). After being set with a designed laser pulse energy, which is achieved with a quartz half-wave plate and a Glan–Taylor polarizer, the laser beam is transformed into a Bessel beam and a following ring-like beam by an axicon. Then, a combination of a lens and an objective is used to generate the final donut focus. The apex angle and reflective index of the axicon are 175° and 1.511, respectively. The focal length of the lens is 150 mm, and the numerical aperture (NA) is 0.25 for the objective of 10 times magnification. It should be noted that the objective must be put in front of the focal plane of the lens. The optical axis of the final donut-shaped beam is perpendicular to the surface of samples (polymethyl methacrylate, PMMA), and the donut focus locates on the samples' front surface. The samples and a sample holder are mounted on a three-dimensional linear translation stage. During the fabrication process, the sample is moved in the plane where the donut focus is located. As a comparison, a cylindrical lens is employed to directly focus the original output Gaussian beam to ablate samples. After irradiation with the donut-shaped beam and the cylindrical lens focused beam, a confocal laser scanning microscope (CLSM) and a metallographic microscope are used to characterize the fabricated microstructures.

Experimentally, a plane can be produced directly by the donut-shaped beam with one scanning, as shown in Fig. 2(a). The used laser pulse energy and scanning speed are 500 μJ/pulse and 0.8 mm/s, respectively. Based on the parameters of pulse repetition rate, scanning speed, and ablated line width with a single pulse (about 10.5 μm for pulse energy of 500 μJ/pulse), we can calculate the overlap ratio of two adjacent pulses, which is about 92.4% with the scanning speed of 0.8 mm/s. It can be seen that the treated surface maintains a relatively high level of flatness, which indicates that the spatial intensity distribution of the finally formed laser beam has a flat top, at least from the side view. This can be better illustrated by the cross-sectional profile of the polished surface, as shown in Fig. 2(c). The experimental result is in good agreement with the theoretical analysis of the donut-shaped beam, as we discussed above. As a comparison, a transverse line-focus created by a cylindrical lens is also employed to implement the experiment of plane processing. To produce a similar level of surface structures, a pulse energy of 600 μJ/pulse and a scanning speed of 1 mm/s are used. The machined result is shown in Fig. 2(b). Though large-area material can also be removed directly by this approach, the surface is definitely not a flat plane. Since most of the laser energy still gathers in the central area for such a directly focused beam, the shape of the treated area is an obvious groove with the

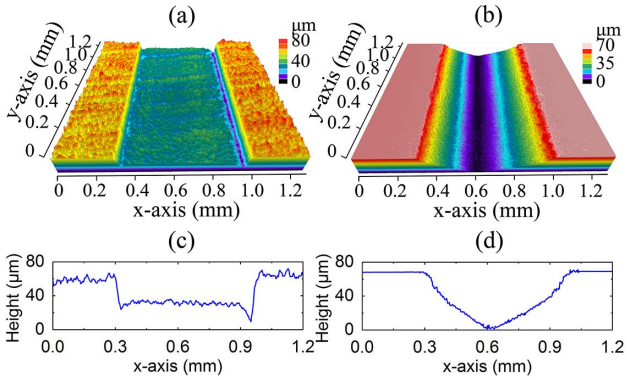

Fig. 2. CLSM images of fs laser fabrication by (a) an axicon-generated donut-shaped beam and (b) a cylindrical directly focused beam. (c),(d) The corresponding cross-sectional profiles.

depth increasing gradually to the maximum from both edges to the center, as the cross-sectional image shown in Fig. 2(d). Thus, it is unsuitable for highly-efficient plane processing by a donut-shaped beam.

To apply the ability of the donut-shaped beam in highly-efficient plane processing, laser polishing is performed in this work. The influence of scanning speed, laser pulse energy, and scanning times on the roughness of polished surfaces is systematically discussed. Figure 3 shows polished surfaces with different scanning speeds of 0.1, 0.2, 0.4, 0.6, 0, 1.0, 1.2, and 1.4 mm/s, respectively. The used laser pulse energies for these polished surfaces are 500 μJ/pulse, and all of them are polished with only one scanning. The original roughness of the surface is 3.38 μm. It can be seen from Fig. 3 that the roughness is decreased with the scanning speed increasing. Its variation tendency is illustrated in Fig. 4(a) by the blue line with triangles. It shows that the roughness reaches the minimum after the scanning speed is enhanced to 0.8 mm/s and then remains almost unchanged. For different laser pulse energies, the variation tendency is the same, but the inflection point has a left-shift for low laser pulse energies. Like the laser pulse energy of 300 μJ/pulse in Fig. 4(a) of the black line with squares, it is at 0.4 mm/s of the scanning speed when the roughness reaches the minimum. However, the effect of the laser pulse energy on the roughness of processed surfaces is a little complicated. As shown in Fig. 4(a), the roughness is increased with the laser pulse energy when the scanning speed is less than 0.6 mm/s, while the surface roughness treated with the laser pulse energy of 400 μJ/pulse is always better than that with 300 and 500 μJ/pulse when the scanning speed exceeds 0.6 mm/s. For the scanning times, the roughness appears to be worse with it added, as shown in Fig. 4(b).

The minimal roughness that has been reached in this work is 1.4 μm. Actually, it is not a very satisfying result compared with laser polishing results discussed in other papers[22–24]. The main reason is the used laser system. Here, a fs laser is employed, since there is only a fs laser system in our laboratory. Generally, a low level of surface roughness processed by a fs laser is hard to reach because the ablation mechanism of the fs laser is mainly the coulomb explosion, and a large number of microstructures will be formed in the treated area. If a nanosecond (ns) laser can be employed to polish again, as the thermal effect is significant during the ns laser fabrication process, most of the microstructures will be melted, and the roughness will be improved dramatically. In this Letter, we mainly focus on demonstrating the ability of the donut-shaped beam in highly-efficient plane processing.

Another advantage of the proposed approach for highly-efficient plane processing is that the scanning width, i.e., the diameter of the final donut focus, can be varied continuously by adjusting the relative distance L between the lens and the objective, as shown in Fig. 1(a). For the ring-like beam, behind the Bessel area are two collimated plane waves with a certain angle θ in any axial section, where the diameter D' of the donut focus created by the lens is a fixed value. To make the diameter D of the finally formed donut focus adjustable and to further enhance the laser intensity at the focus, the objective is employed. Based on the geometrical optics, the relationship between the scanning width and the distance L can be described as

$$D = 2f_1 f_2 \tan\theta/(f_1 + f_2 - L), \tag{2}$$

where f_1 and f_2 are the focal lengths of the lens and the objective, respectively. Given $f_1 = 150$ mm, $f_2 = 8$ mm, and $\theta = 1.28°$, we have their relationship shown in Fig. 5. It can be seen that the scanning width can be varied from about 0.3 mm to near 1.5 mm by changing the relative distance L from zero to 120 mm. Moreover, the range can be further extended by using a lens or an objective with different focal lengths.

In this Letter, we demonstrate a simple method for highly-efficient plane processing, fully based on fs laser

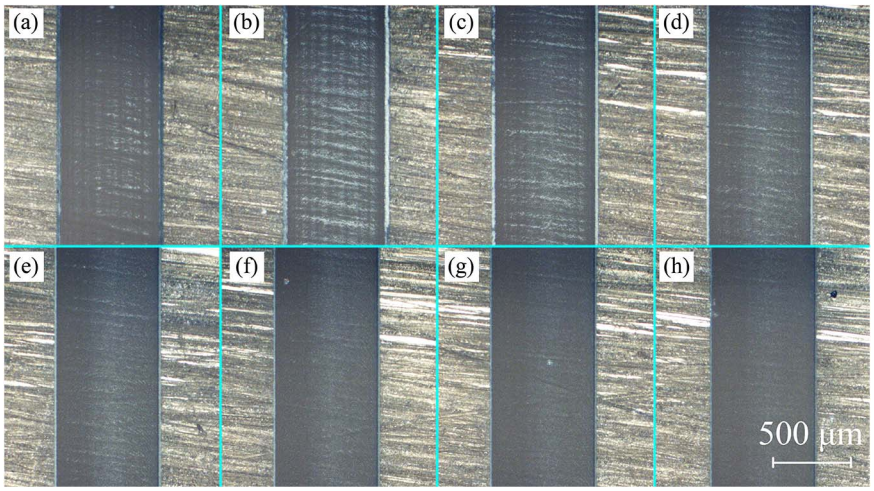

Fig. 3. Donut-shaped beam polished surfaces with different scanning speeds. (a) 0.1 mm/s, (b) 0.2 mm/s, (c) 0.4 mm/s, (d) 0.6 mm/s, (e) 0.8 mm/s, (f) 1.0 mm/s, (g) 1.2 mm/s, and (h) 1.4 mm/s.

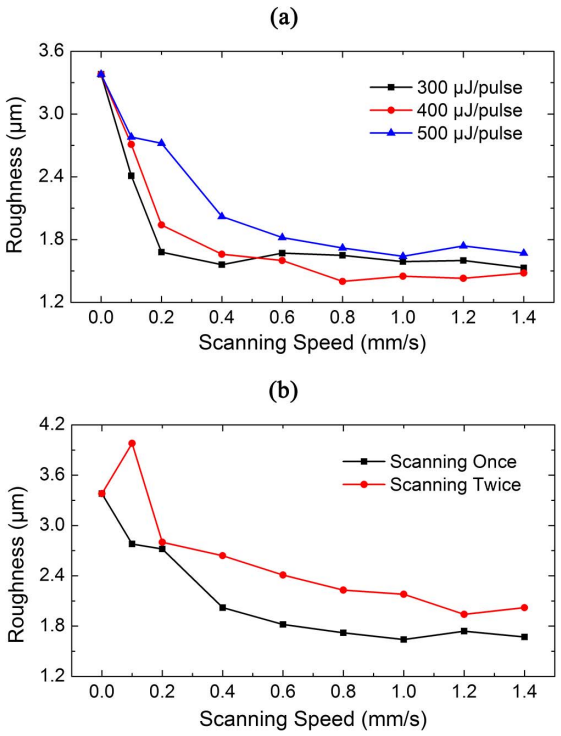

Fig. 4. Influence of (a) the scanning speed and the laser pulse energy, and (b) the scanning times on the roughness of processed surfaces by the donut-shaped beam.

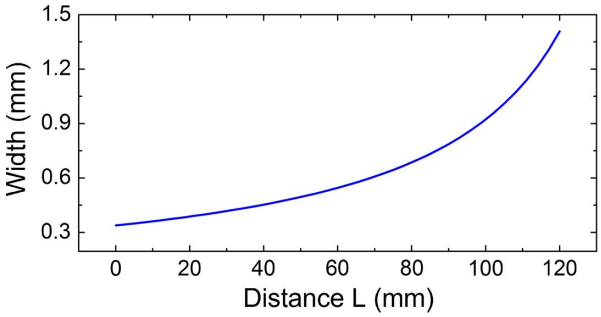

Fig. 5. Relationship between the scanning width and the relative distance from the lens to the objective.

beam shaping. The laser with a Gaussian distribution is converted to a spatial donut shape. Numerical simulation indicates that the central intensity of the donut-shaped beam is evenly distributed along the donut contour, and it seems like a flat top from the side view. By applying the donut-shaped beam to the polishing experiments, planes with a high level of flatness are obtained directly with only one scanning, and the surface roughness is improved significantly. Moreover, we find that the roughness of polished surfaces is mainly affected by the scanning speed, the laser pulse energy, and the scanning times. The roughness is improved with the scanning speed increasing to a steady value, and the laser pulse energy of 400 μJ/pulse and one scanning can give us a better result. Besides, the scanning width, i.e., the diameter of the donut-shaped focus, can be controlled in the range of about 0.3 mm to near 1.5 mm by adjusting the relative distance between the lens and the objective.

This work was supported by the National Key R&D Program of China (No. 2017YFB1104300), the National Natural Science Foundation of China (NSFC) (No. 51505505), the Hunan Provincial Innovation Foundation for Postgraduate (No. CX2015B044), the Natural Science Foundation of Hunan Province (No. 2016JJ3147), the Open Research Fund of Key Laboratory of High Performance and Complex Manufacturing, Central South University (No. KFKT2015-09).

References

1. J. H. McLeod, J. Opt. Soc. Am. **44**, 592 (1954).
2. C. B. Burckhardt, H. Hoffmann, and P. A. Grandchamp, J. Acoust. Soc. Am. **54**, 1628 (1973).
3. Z. Jaroszewicz, A. Burvall, and A. T. Friberg, Opt. Photon. News **16**, 34 (2005).
4. Z. Luo, J. Duan, and C. Guo, Opt. Lett. **42**, 2358 (2017).
5. J. Zheng, B. Yao, Y. Yang, M. Lei, P. Gao, R. Li, S. Yan, D. Dan, and T. Ye, Chin. Opt. Lett. **11**, 112601 (2013).
6. R. Arimoto, C. Saloma, T. Tanaka, and S. Kawata, Appl. Opt. **31**, 6653 (1992).
7. S. M. Perinchery, A. Shinde, C. Y. Fu, X. J. J. Hong, M. Baskaran, T. Aung, and V. M. Murukeshan, Sci. Rep. **6**, 30844 (2016).
8. Z. Zhai, Q. Lv, X. Wang, L. Yang, Z. Xu, and H. Tao, in *4th International Conference on Photonics, Optics and Laser Technology*, IEEE (2016), p. 1.
9. D. Lorenser, C. C. Singe, A. Curatolo, and D. D. Sampson, Opt. Lett. **39**, 548 (2014).
10. J. Arlt, V. Garces-Chavez, W. Sibbett, and K. Dholakia, Opt. Commun. **197**, 239 (2001).
11. S. Cabrini, C. Liberale, D. Cojoc, A. Carpentiero, M. Prasciolu, S. Mora, V. Degiorgio, F. De Angelis, and E. Di Fabrizio, Microelectron. Eng. **83**, 804 (2006).
12. L. Zhao, F. Wang, L. Jiang, Y. Lu, W. Zhao, J. Xie, and X. Li, Chin. Opt. Lett. **13**, 041405 (2015).
13. Y. Yu, L. Jiang, Q. Cao, B. Xia, Q. Wang, and Y. Lu, Opt. Express **23**, 32728 (2015).
14. X. Dong, Z. Xie, Y. Song, K. Yin, D. Chu, and J. Duan, Chin. Opt. Lett. **15**, 090602 (2017).
15. D. Chu, K. Yin, X. Dong, Z. Luo, Y. Song, and J. Duan, Chin. Opt. Lett. **16**, 11401 (2018).
16. Q. Wang, L. Jiang, J. Sun, C. Pan, W. Han, G. Wang, H. Zhang, C. P. Grigoropoulos, and Y. Lu, Photon. Res. **5**, 488 (2017).
17. Y. Ju, C. Liu, Y. Liao, Y. Liu, L. Zhang, Y. Shen, D. Chen, and Y. Cheng, Chin. Opt. Lett. **11**, 072201 (2013).
18. H. Xia, J. Wang, Y. Tian, Q. D. Chen, X. B. Du, Y. L. Zhang, Y. He, and H. B. Sun, Adv. Mater. **22**, 3204 (2010).
19. Y. C. Guan, G. K. L. Ng, H. Y. Zheng, M. H. Hong, X. Hong, and Z. Zhang, Appl. Surf. Sci. **270**, 526 (2013).
20. A. V. Rode, D. Freeman, K. G. H. Baldwin, A. Wain, O. Uteza, and P. Delaporte, Appl. Phys. A-Mater. Sci. Process. **93**, 135 (2008).
21. Z. Luo, C. Wang, J. A. Duan, X. Sun, Y. Hu, and K. Yin, Appl. Opt. **54**, 3943 (2015).
22. T. L. Perry, D. Werschmoeller, X. Li, F. E. Pfefferkorn, and N. A. Duffie, J. Manuf. Process. **11**, 74 (2009).
23. C. Nüsser, I. Wehrmann, and E. Willenborg, Phys. Procedia **12**, 462 (2011).
24. T. L. Perry, D. Werschmoeller, X. Li, F. E. Pfefferkorn, and N. A. Duffie, J. Manuf. Sci. Eng. **131**, 031002 (2009).